AMERICAN SOCIETY FOR MICROBIOLOGY | Journal of Virology

Virology | Full-Length Text

The HTLV-I oncoprotein Tax inactivates the tumor suppressor FBXW7

Marcia Bellon,[1] Chien-hung Yeh,[1] Xue Tao Bai,[1] Christophe Nicot[1]

AUTHOR AFFILIATION See affiliation list on p. 13.

ABSTRACT Human T-cell leukemia virus type 1 (HTLV-I) is the etiological agent of adult T-cell leukemia (ATL). Mutational analysis has demonstrated that the tumor suppressor, F-box and WD repeat domain containing 7 (FBXW7/FBW7/CDC4), is mutated in primary ATL patients. However, even in the absence of genetic mutations, FBXW7 substrates are stabilized in ATL cells, suggesting additional mechanisms can prevent FBXW7 functions. Here, we report that the viral oncoprotein Tax represses FBXW7 activity, resulting in the stabilization of activated Notch intracellular domain, c-MYC, Cyclin E, and myeloid cell leukemia sequence 1 (BCL2-related) (Mcl-1). Mechanistically, we demonstrate that Tax directly binds to FBXW7 in the nucleus, effectively outcompeting other targets for binding to FBXW7, resulting in decreased ubiquitination and degradation of FBXW7 substrates. In support of the nuclear role of Tax, a non-degradable form of the nuclear factor kappa B subunit 2 (NFκB2/p100) was found to delocalize Tax to the cytoplasm, thereby preventing Tax interactions with FBXW7 and Tax-mediated inhibition of FBXW7. Finally, we characterize a Tax mutant that is unable to interact with FBXW7, unable to block FBXW7 tumor suppressor functions, and unable to effectively transform fibroblasts. These results demonstrate that HTLV-I Tax can inhibit FBXW7 functions without genetic mutations to promote an oncogenic state. These results suggest that Tax-mediated inhibition of FBXW7 is likely critical during the early stages of the cellular transformation process.

IMPORTANCE F-box and WD repeat domain containing 7 (FBXW7), a critical tumor suppressor of human cancers, is frequently mutated or epigenetically suppressed. Loss of FBXW7 functions is associated with stabilization and increased expression of oncogenic factors such as Cyclin E, c-Myc, Mcl-1, mTOR, Jun, and Notch. In this study, we demonstrate that the human retrovirus human T-cell leukemia virus type 1 oncoprotein Tax directly interacts with FBXW7, effectively outcompeting other targets for binding to FBXW7, resulting in decreased ubiquitination and degradation of FBXW7 cellular substrates. We further demonstrate that a Tax mutant unable to interact with and inactivate FBXW7 loses its ability to transform primary fibroblasts. Collectively, our results describe a novel mechanism used by a human tumor virus to promote cellular transformation.

KEYWORDS FBXW7, HTLV, Notch, MYC, Cyclin E, Mcl-1, ATL, Tax, CDC4, IKK, NF-kB, leukemia

Human T-cell leukemia virus type 1 (HTLV-I) is a complex human retrovirus etiologically linked to adult T-cell leukemia (ATL), lymphoma, and HTLV-I-associated myelopathy/tropical spastic paraparesis. The prognosis of the disease is influenced by multiple factors, including the specific HTLV-I viral subtype, the expression patterns of viral genes, and various host-related elements, such as the complexity of the host immune response to the invading virus (1–3). Genomic and epigenetic changes found in

Editor Frank Kirchhoff, Ulm University Medical Center, Ulm, Germany

Address correspondence to Christophe Nicot, cnicot@kumc.edu.

The authors declare no conflict of interest.

See the funding table on p. 13.

Received 28 February 2024
Accepted 17 May 2024
Published 14 June 2024

HTLV-I-infected cells are also associated with disease progression (4–6). The Tax protein of HTLV-I plays a crucial role in the onset of ATL (7, 8) and employs a "random mutagenesis" model to achieve an oncogenic state (9). Tax utilizes various mechanisms, including increasing NF-κB (nuclear factor of kappa light polypeptide gene enhancer in B-cells) activity, controlling the cell cycle, interfering with DNA repair, and altering cell cycle checkpoints and apoptosis regulators (7, 10–13).

Our previous findings indicate that approximately 25% of all ATL patients have mutations in F-box and WD repeat domain containing 7 (FBXW7) (14). An analysis of the COSMIC (catalog of somatic mutations in cancer) database showed that the overall mutational rate of FBXW7 in all human tumors is nearly 8% (15). FBXW7 is a tumor suppressor that functions in the phosphorylation-dependent ubiquitination of target proteins harboring a CPD (CDC4 phosphodegron) sequence (16, 17). Known substrates include master regulators of cellular proliferation, including oncogenes: Notch, Cyclin E, c-Myc (MYC proto-oncogene, BHLH transcription factor), Mcl-1 (MCL1 apoptosis regulator, BCL2 family member), mTOR (mechanistic target of rapamycin kinase), c-Jun (Jun proto-oncogene, AP-1 transcription factor subunit), and BRAF (B-Raf proto-oncogene, serine/threonine kinase) (18–21). Target substrates are phosphorylated on the CPD by GSK3-β (glycogen synthase kinase 3 beta) and CDK2 (cyclin-dependent kinase 2) to promote interactions with FBXW7 (22, 23). Once bound, FBXW7 recruits the SCF (complex of SKP1, CUL1, and F-box protein) ubiquitin ligase complex, leading to ubiquitination and degradation by the proteasome (23). This facilitates the degradation of highly oncogenic substrates, such as c-MYC and activated Notch, thereby inhibiting cellular transformation. Several known substrates of FBXW7 are relevant to HTLV-I pathobiology. Notch1, c-MYC, Cyclin E, p53, and Mcl-1 are all overexpressed in ATL cells, and targeted inhibition of these pathways has been shown to induce rapid apoptosis in HTLV-I-transformed cells (20, 24–27).

Our published data demonstrate that FBXW7 expression is reduced in ATL cells and that both genetic and non-genetic mechanisms are responsible for the inactivation of FBXW7 functions (14). While previous studies have reported a high frequency of mutation at residues R465, R479, and R505 in FBXW7, resulting in a complete loss of substrate interaction, FBXW7 mutations identified in our studies are phenotypically different and demonstrate a selective loss of binding of some but not all FBXW7 targets (14, 28). We have found that specific FBXW7 mutations reduce the binding and degradation of Notch by FBXW7 in ATL patient cells (14). In addition, ATL patients' cells frequently harbor high rates of Notch-1-activating mutations (24). Finally, we also found that Notch signaling can be activated in ATL cells independently of genetic mutation by over-expressing the JAG1 (jagged canonical Notch ligand 1) receptor (29). Therefore, a combination of non-genetic host mechanisms and viral-induced Notch/FBXW7 genetic mutations can over-activate Notch signaling in ATL cells.

FBXW7 inactivation has been linked to the resistance of cancer cells to drug therapy, microtubule-targeting agents, and anti-PD1 immunotherapies (30–32). Furthermore, FBXW7 plays a key role in preserving genome integrity. In response to DNA damage, FBXW7 is recruited to DSB where it ubiquitinates XRCC4 (X-ray repair cross complementing 4) and stimulates DNA repair (33). Furthermore, FBXW7 targets the degradation of factors such as Cyclin E, AURKA (aurora kinase A), and c-Myc, which have been implicated in supernumerary centrosomes and genome instability (34, 35). These functions are clearly in opposition to Tax functions in HTLV-I-infected cells. For instance, Tax was shown to localize to centrosomes during mitosis and induced supernumerary centrosomes (36). Tax impairs DNA replication forks, resulting in the accumulation of DSBs, and simultaneously, Tax-mediated NF-κB activation was associated with the inhibition of HR DNA repair (11, 37). In this study, we report that HTLV-I Tax interacts with and inactivates the tumor suppressor FBXW7, resulting in elevated expression of oncogenic proteins such as Notch intracellular domain (NICD), c-MYC, Cyclin E, and MCL1. In contrast, HTLV-I HBZ protein did not affect FBXW7. Using specific mutants, we further demonstrate that neither the activation of the CREB (cAMP responsive element binding protein) nor the

NF-κB pathway is solely responsible for FBXW7 inactivation. Although Tax expression led to the stabilization of FBXW7, the latter did not influence Tax expression levels. Moreover, a Tax mutant incapable of interacting with FBXW7 failed to hinder its functions and exhibited diminished transforming activities. These findings suggest that Tax-mediated inactivation of FBXW7 is a pivotal event in the HTLV-I transformation process.

MATERIALS AND METHODS

Cell lines and plasmids

HTLV-I cell lines, MT4, C91PL, and C8166, and T-cell line, Jurkat, were maintained in RPMI (Roswell Park Memorial Institute medium) and obtained from the ATCC (38–40). 293T and Rat1 cells were maintained in DMEM (Dulbecco's modified Eagle medium). All media were supplemented with 10% FBS (fetal bovine serum). Cyclohexamide was added at 100 µg/mL for indicated times. Protein half-life was determined through the quantification of western blot bands by ImageJ software. The following plasmids were used: pcTax, Flag-FBXW7, myc-NICD, HA-Mcl-1, HA-c-MYC, HA-HBZ was cloned into the pSI-H1 vector, pCDNA-G148V Tax, pcDNA-M47 Tax, p65DN [gift from W. C. Greene (41)], p100DN [gift from Gutian Xiao (42)], IKKα K44M [gift from Richard B. Gaynor (42, 43)], HA-tagged Ub (K48) [gift from Edward W. Harhaj (44)], and Tax-GFP vector [gift from R. Mahieux (45)]. GSK3β was cloned into the UBC vector. Site-directed mutagenesis was performed to introduce the mutation S9A, using the QuikChange Mutagenesis Kit (Stratagene).

Generation of Tax mutants

Tax-J was derived from the Tax mutant, JPXM, inducible cell line (46). The QuikChange II Site-directed Mutagenesis Kit (Stratagene) was used on 0.025 µg of pcTax to generate Tax mutants: addition of Ser63, and mutations of R222K, L308H, Ser63/R222K (2T-R222K), Ser63/L308H (2T-L308H), and Ser63/R222K/L308H (TaxM3). Sequencing of wild-type pcTax demonstrated a methionine to isoleucine mutation at position 206 (M206I), which was replicated in all newly generated mutants. Appropriate Tax-mutagenized primers were generated for Tax mutants, and PCR was performed according to the manufacturer's instructions. DNA was digested with DpnI and transformed into XL1 Blue competent cells. Positive colonies were amplified, and DNA was purified and subsequently sequenced to verify mutations. For double and triple Tax mutants, one mutation was made at a time, sequenced, and then plasmid DNA was subsequently used as a template for the second or third mutations.

Transfections, western blots, nuclear/cellular extraction, and immunoprecipitation

Transient transfection assays were performed in 293T or Rat1 cell lines. Cells were transfected with Polyfect Transfection Reagent (Qiagen) or calcium phosphate (Invitrogen). Lysates were collected after 24 hours for c-MYC and Mcl-1 or 48 hours for Notch and Cyclin E. Cells were lysed in RIPA lysis buffer [Tris-HCl: 50 mM, pH 7.4, NaCl 150 mM, 1% NP-40, 0.5% sodium deoxycholate, 0.1% sodium dodecyl sulfate (SDS), EDTA 1 mM, 10 mg/mL phenylmethylsulfonyl fluoride, aprotinin (2 µg/mL), and 100 mM sodium orthovanadate], and cell lysates were separated by sodium dodecyl sulfate-polyacrylamide gel electrophoresis (SDS-PAGE). Primary antibodies used were as follows: myc (9E10) (Owl Laboratories), Flag (M2; Sigma), HA (3F10; Roche), Actin (C-4), Tax (1A3), Cyclin A and NF-κB p52 (C5; Santa-Cruz), GSK3β (Cell Signaling), and FBXW7 (Proteintech and Santa-Cruz). When possible, blots were stripped and re-probed for loading controls. Cytoplasmic and nuclear extracts were obtained by lysing cells in hypotonic lysis buffer (10 mM HEPES, pH 7.9, 1 mM $MgCl_2$, 0.5 mM NaCl, and 0.5% NP-40) and hypertonic buffer (5 mM HEPES, pH 7.9, 5 mM $MgCl_2$, 0.1 mM EDTA, 0.4 M NaCl, and 1 mM DTT), respectively. Cyclin A was used as a control. For immunoprecipitations, whole cell lysates

or transfected lysates were prepared in NP-40 lysis buffer (150 mm KCl, 10 mM Tris, pH 8.8, 5 mM $MgCl_2$, and 0.65% NP-40). An equal amount of cell lysates were pre-cleared and then immunoprecipitated with the appropriate antibody overnight at 4°C. Lysates were then mixed with recombinant protein A/G beads (MicroProtein Technologies) for 2 hours, washed, and resuspended in 2× SDS-protein loading buffer. Non-immunoprecipitated protein lysates served as controls.

Green fluorescent protein analysis

293T cells were transfected with Tax-GFP (45) and/or p100DN plasmids. At 48 hours post-transfection, cells were washed in PBS and fixed on coverslips with 4% paraformaldehyde (Electron Microscopy Sciences). Cells were washed in PBS, and cell nuclei were stained with DAPI (4′,6′-diamine-2 phenylindole dihydrochloride). Cells were washed in PBS and mounted with the anti-fade reagent, 1, 4-diazobicyclo-(2,2,2)-octane (DABCO). Images were taken on a Nikon 80i microscope with a 40× objective, using a Nikon Digital slight DS-Fi3 8bt color camera. Images are representative of the whole experiment.

GST pull-down

Glutathione S-transferase (GST)-fused proteins were obtained from pGEX (empty vector), and pGEX-Tax bacterial cultures were purified with Glutathione Sepharose 4B (GE Healthcare), according to standard protocols. 293T cells in a 10-cm dish were transfected by calcium phosphate with 15 µg pcDNA control or Flag-FBXW7, and 48 hours later, cells were lysed and mixed with purified glutathione S-transferase or GST-Tax. Following pull-down and washes, proteins were eluted using GST elution buffer (50 mM Tris-HCl and 10 mM reduced glutathione, pH 8.0). Lysates were separated on SDS-PAGE gels and probed with GST (G-7781, Sigma), Tax, or FLAG antibodies.

Luciferase assays

293T cells were transfected with pc-Tax, mutant Tax, FLAG-FBXW7, p65DN, p100DN, IKKαDN, and NF-κB-Luc (47) or HTLV-LTR-I (48) luciferase plasmids using Polyfect (Qiagen). pCDNA was used as a negative control. Cell extracts were lysed in 1× passive lysis buffer (Promega) and analyzed using the Luciferase Reporter Assay System (Promega), according to the manufacturer's instructions. Luciferase assays were performed at least twice from independent transfection experiments. Luciferase was measured on a Junior LB9509 instrument (Berthold Technologies).

Colony formation assay

Rat1 cells were transfected in duplicate with pCDNA, pcTax, Tax mutants, and pSIH1-puro plasmids. At 48 hours post-transfection, media were removed and replaced with DMEM containing puromycin. Cells were selected over several weeks until discernible colonies formed. Cells were washed in PBS, fixed with 4% paraformaldehyde, washed in distilled water, and stained overnight with Coomassie blue reagent, and colonies were photographed. Colonies were counted from at least two transformation assays.

RESULTS

We have previously shown that ATL patient tumor cells carry oncogenic mutations resulting in constitutive activation of Notch signaling and loss of function of FBXW7 (14, 24). Additional studies from our laboratory also found activation of Notch signaling without genetic mutations, suggesting the existence of additional mechanisms (29). Since HTLV-I Tax can prevent the function of multiple tumor suppressors from activating oncogenic pathways (7), we investigated the effect of Tax expression on NICD and MYC protein expression levels. Our studies revealed that Tax expression significantly increases the levels of Notch and c-MYC protein expression. To gain further insights, we examined whether Tax expression may affect the degradation and half-life of these

proteins. Transient transfection assays and cycloheximide chase treatments confirmed that Tax expression significantly extended the half-life of both NICD (from 30 minutes to >3 hours) and Myc (from 22 minutes to 79 minutes) (Fig. 1A). This is consistent with our previous work, which demonstrated that NICD has a half-life of approximately 1.5 hours in normal peripheral blood mononuclear cells (PBMCs) but is extended to over 3 hours in HTLV-I cells (24). Since both oncogenes are targeted by FBXW7 for proteasomal degradation, we next examined whether Tax could prevent FBXW7-mediated degradation of NICD and c-MYC. To this end, we co-expressed MYC-tagged NICD and flag-tagged FBXW7 in the presence or absence of a Tax expression vector. As expected, exogenous FBXW7 induced degradation of NICD and c-MYC, as demonstrated by reduced expression levels in western blotting experiments (Fig. 1B). Nevertheless, the existence of Tax substantially hindered FBXW7's capacity to prompt degradation, leading to not only a full recovery of expression levels but also enhanced expression of NICD and c-MYC (Fig. 1B). Furthermore, we demonstrate that Tax also prevented FBXW7-mediated degradation of additional known targets Cyclin E and Mcl-1 (Fig. 1B), two proteins important for the HTLV-I oncogenesis process. Our studies show that a dose-dependent increase of FBXW7 expression was not able to target Tax for degradation (Fig. 1C). Since Tax transcriptional activities have been shown to be important for the inactivation of tumor suppressors such as p53, we next investigated whether FBXW7 expression may affect Tax transcriptional activities through the CREB and NF-κB pathways. Our luciferase data show that

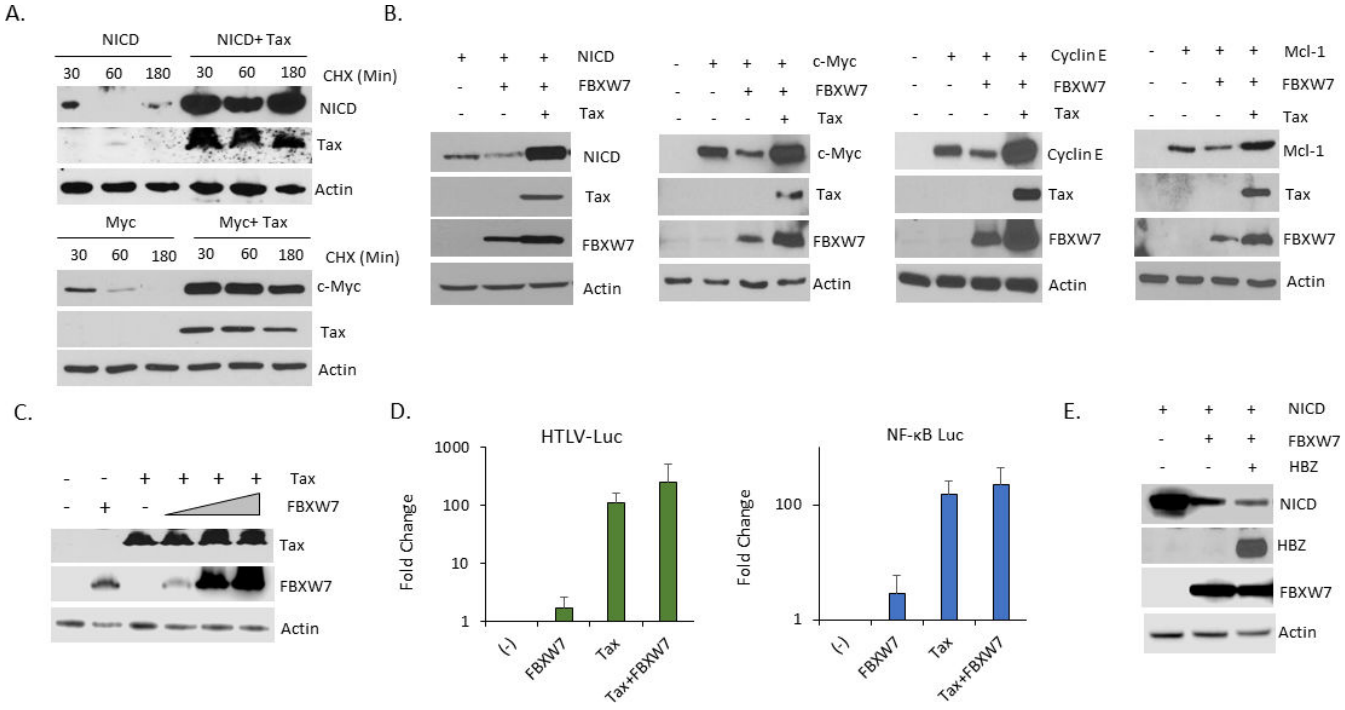

FIG 1 HTLV-I Tax inhibits FBXW7-mediated degradation of target proteins. (A) 293T were transfected with Tax (0.5 µg) and myc-NICD (0.16 µg) or HA-c-MYC (0.25 µg) for 48 hours. Before collection, cells were treated with 10 µg/mL cycloheximide (CHX) for 30, 60, or 180 minutes. c-Myc half-life increased from 22 minutes to 79 minutes in the presence of Tax. NICD half-life increased to over 3 hours in the presence of Tax. (B) Tax expression prevents FBXW7-mediated degradation of NICD, c-MYC, cyclin E, and Mcl-1. 293T cells were transfected with 0.50 µg pcTax, 0.16 µg myc-NICD, and 2.0 µg Flag-FBXW7. Cell lysates were collected 48 hours later. 293T cells were transfected with 0.50 µg pcTax, 0.25 µg HA-c-Myc, and 2.0 µg Flag-FBXW7. Cell lysates were collected 24 hours later. 293T cells were transfected with 0.50 µg pcTax, 0.15 µg myc-Cyclin E, and 2.0 µg Flag-FBXW7. Cell lysates were collected 48 hours later. 293T cells were transfected with 0.50 µg pcTax, 0.2 µg HA-Mcl-1, and 2.0 µg Flag-FBXW7. Cell lysates were collected 24 hours later. Actin served as a loading control. (C) Tax is not a target of FBXW7-mediated inhibition. 293T cells were transfected with pcTax (0.5 µg), along with increasing doses of Flag-FBXW7 (0.5–2.0 µg). Forty-eight hours later, lysates were analyzed for Tax and FBXW7 expression. (D) 293T were transfected with either NF-κB or HTLV-I luciferase plasmids (0.5 µg) along with pcTax (0.5 µg) and/or Flag-FBXW7 (1.0 µg). Twenty-four hours later, lysates were collected for luciferase assays. Fold change was calculated based on empty vector control. (E) HTLV-I HBZ cannot inhibit FBXW7 activities. 293T cells were transfected with pcTax (0.5 µg) or HA-HBZ along with myc-Cyclin E (0.1 µg) or myc-NICD (0.16 µg). Cell lysates were collected 48 hours later. Actin served as a loading control.

FBXW7 does not significantly impact the ability of Tax to stimulate the CREB/ATF or NF-κB signaling pathways (Fig. 1D). Finally, inactivation of FBXW7 was specific to Tax, as HBZ, a latent HTLV-I oncogene, was unable to rescue FBXW7-mediated degradation of NICD (Fig. 1E). These data suggest that Tax-mediated inhibition of FBXW7 may be necessary in the early transformation steps of the virus.

Previous studies have demonstrated that the strength of the interaction between targets and FBXW7 is dependent on the phosphorylation of the CPD by GSK3 kinase (18, 23, 49). Furthermore, several studies have reported that Tax can activate AKT, resulting in strong inhibition of GSK3 activity (50, 51). Finally, Tax has been previously shown to bind directly to tumor suppressors or transcriptional coactivators CBP/p300 to prevent the recruitment and activation of c-MYB (MYB proto-oncogene, transcription factor) (52). These observations suggest that Tax may block FBXW7 interactions with its targets to prevent their degradation, either by inhibiting GSK3 beta or by competitively binding to FBXW7 and preventing the recruitment of potential targets.

To demonstrate potential interactions between Tax and FBXW7, we performed transient transfection assays and co-immunoprecipitation of FBWX7. Results from these assays demonstrated that Tax could indeed interact with FBXW7 in transfected cells (Fig. 2A). Tax is a potent activator of NF-κB and CREB signaling pathways, and many functions of Tax have been assigned to the activation of one or the other (53). We capitalized on well-characterized Tax mutants, M47, defective in Tax-mediated CREB activation, and G148V, which lacks Tax-mediated NF-κB activation, to investigate if specific activities of Tax would be important to inactivate FBXW7 (54, 55). As demonstrated in Fig. 2A, both of these Tax mutants retained the ability to interact with FBXW7, underscoring that CREB and NF-κB activities are dispensable for Tax binding to FBXW7 (Fig. 2A). To determine if Tax could directly bind FBXW7, we used bacterially purified GST-Tax and GST control mixed with cellular extracts from FBXW7-transfected cells. Using GST-pulldown assays, we demonstrated GST-Tax but not the GST control specifically interacted with FBXW7 (Fig. 2B). Importantly, we also confirmed interactions between endogenous Tax and endogenous FBXW7 in co-immunoprecipitation assays of HTLV-I transformed cell lines, C8166, MT4, and C91PL (Fig. 2C). Our studies found that endogenous FBXW7 specifically binds to Tax, while no signal was detected for FBXW7 in the immunoprecipitate of the Tax-negative, human T-cell line, Jurkat (Fig. 2C). Together, these results demonstrate that Tax interacts with FBXW7. We next investigated whether Tax interaction with FBXW7 may compete with the binding and recruitment of FBXW7 targets for degradation. To this end, we performed transient transfection assays of NICD and FBXW7 in the presence or the absence of Tax and immunoprecipitated NICD to evaluate the amount of bound FBXW7. As demonstrated by the results presented in Fig. 2D, the amount of FBXW7 bound to NICD was significantly decreased when Tax was coexpressed. Consistent with these results, ubiquitination levels of both NICD and c-MYC were significantly reduced in the presence of Tax expression (Fig. 2E), suggesting that Tax binding to FBXW7 prevents the recruitment and degradation of its targets (Fig. 2E). In addition to the competitive binding of FBXW7, Tax may also prevent the recruitment of FBXW7 targets by interacting with specific targets and masking the FBXW7 binding site or altering their conformation thereby preventing ubiquitination. Thus, we next investigated the binding of Tax to NICD and c-MYC in transient transfection assays. As shown in Fig. 2F, co-immunoprecipitation confirmed the binding of Tax to NICD or c-MYC. These data are consistent with a previous report showing Tax can interact with NICD (56) and suggest that Tax can also bind FBXW7 substrates preventing them from being assembled into an FBXW7 complex.

Since GSK3-mediated phosphorylation of the CPD is required for interaction with FBXW7, and since Tax can activate AKT signaling resulting in the inactivation of GSK3, we next tested whether Tax-mediated inactivation of GSK3 was required for blocking FBXW7 functions (22, 51, 57). We performed transient transfection assays of NICD, FBXW7, and Tax as described in Fig. 2 in the presence of wild-type GSK3β or in the presence of a constitutively active GSK3β (S9A) that cannot be blocked by Tax. Results from these studies showed that even in the presence of a constitutively active GSK3β, Tax can still

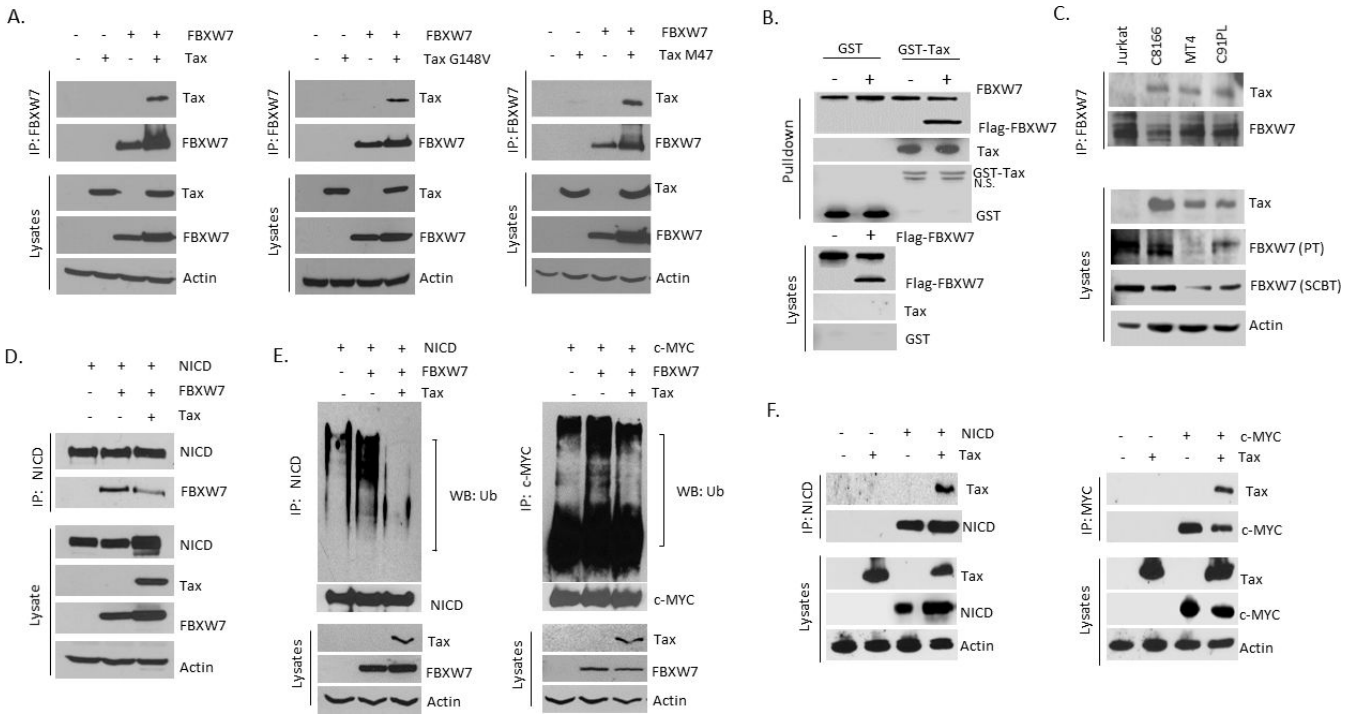

FIG 2 Tax binds directly to FBXW7 and retains Tax activity. (A) Tax binds FBXW7, independent of NF-κB or CREB/ATF activity. 293T cells were transfected with Flag-FBXW7 along with wild-type (A), NF-κB-deficient (G148V) (B), or CREB/ATF-deficient (M47) (C) Tax (0.5 µg). Forty-eight hours later, lysates were immunoprecipitated with Flag (FBXW7) antibody and analyzed for Tax binding by western blot. Lysates and actin served as controls. (B) Tax binds directly to FBXW7. 293T cells were transfected with or without Flag-FBXW7 (15 µg). Forty-eight hours post-transfection, cell lysates were incubated overnight with purified GST or purified GST-Tax proteins. The next day, lysates were washed, run on electrophoresis gels, and probed with anti-GST or anti-Flag antibodies. (C) Interaction between endogenous Tax and FBXW7 in HTLV-1 transformed cells. An equal amount of lysates were run to demonstrate loading controls. Jurkat and Tax-positive C91PL, MT4, and C8166 cells were lysed in NP40 lysis buffer, and 500 µg was incubated overnight with FBXW7 antibody (Proteintech, PT). Lysates were immunoprecipitated with protein AG beads and separated on SDS-PAGE blots. IPs and lysates were incubated with anti-Tax and anti-FBXW7. Actin served as a control for loading. (D) Tax binding to FBXW7 prevents the recruitment of its targets. Tax decreases the amount of FBXW7 binding to Notch. 293T cells were transfected with pcTax, myc-NICD, and/or Flag-FBXW7. Forty-eight hours later, lysates were collected and immunoprecipitated with myc(NICD) and then analyzed by western blot with Tax, myc, or flag antibodies. Lysates and actin served as controls. (E) Tax prevents FBXW7-mediated ubiquitination of substrates. 293T cells were transfected with pcTax, HA-Ub, myc-NICD, or HA-c-MYC, with or without Flag-FBXW7. Lysates were immunoprecipitated with myc (NICD) or HA (c-MYC), followed by western blot with anti-Ub. Lysates and actin served as controls. (F) Tax binds FBXW7 substrates, Notch, and c-MYC. 293T cells were transfected with pcTax (4 µg) along with myc-NICD (4 µg) or HA-c-MYC (4 µg). Forty-eight hours later, lysates were collected and immunoprecipitated with myc(NICD) or HA(c-MYC) and then analyzed by western blot with Tax, myc, or HA antibodies. Lysates and actin served as controls.

inhibit FBXW7-mediated degradation and stabilize the expression of NICD (Fig. 3A and B).

Activation of the canonical NF-κB pathway is required for the transformation of human primary T-cells by HTLV-I, while activation of the non-canonical NF-κB2 pathway is required for the maintenance of ATL tumor cells (58, 59). We previously demonstrated that Tax-induced NF-κB stimulates the expression of JAG-1 and activation of Notch signaling (29). Previous studies have shown the direct binding of Tax to the IKK (I-kappa-B-kinase) complex components, and we have previously shown that Tax can stimulate hTERT (telomerase reverse transcriptase) enzymatic activity directly through the activation of the IKK complex (60, 61). To investigate the possible role of canonical and non-canonical NF-κB activation in Tax-mediated inhibition of FBXW7, we used dominant negative forms of RelA/p65 and NF-κB2 p100 (42, 62, 63). We first confirmed that all DN mutants acted as expected and effectively inhibited Tax-mediated NF-κB activation in transient luciferase assays (Fig. 3C). Our studies revealed that the expression of RelA/p65 DN or IKKα DN mutants did not affect the ability of Tax to stabilize NICD (Fig. 3D and E). In contrast, the coexpression of NF-κB2 p100 DN completely abolished Tax-mediated

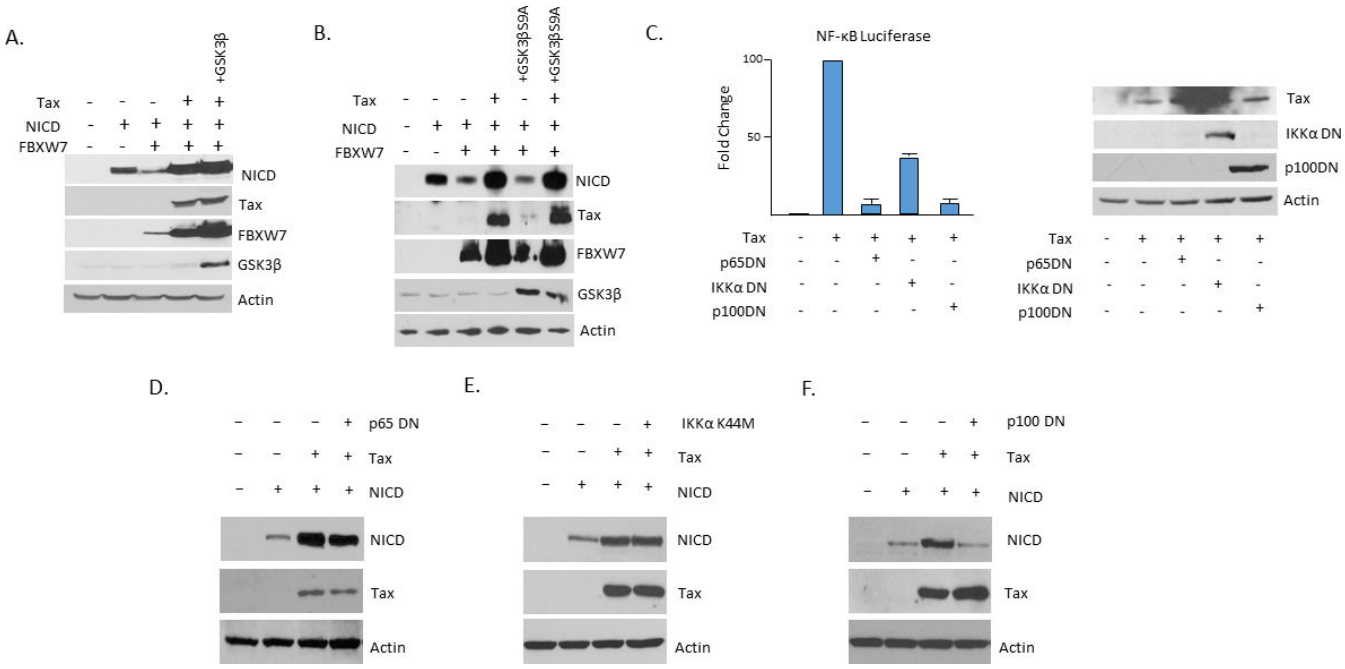

FIG 3 Inactivation of GSK3 activation is not required for Tax-mediated inactivation of FBXW7. (A and B) GSK3β functions are not required for Tax inhibition of FBXW7. 293T cells were transfected with pcTax, (0.5 µg) Flag-FBXW7 (2.0 µg), and myc-NICD (0.16 µg), with or without wild-type GSK3β (A) or mutant GSK3βS9A (1.0 µg) (B). Forty-eight hours later, cells were analyzed by western blot. Actin served as a loading control. (C) 293T cells were transfected with pcTax with or without p65DN, IKKαDN, or p100DN mutants along NF-κB-Luc and RLTK. Luciferase measurements were taken from at least two independent experiments and were normalized to RLTK-renilla luciferase. (D–F) 293T cells were transfected with pcTax, myc-NICD, Flag-FBXW7, and/or p65DN (D), IKKαK44M (E), or p100DN (F) plasmids. Forty-eight hours later, cells were probed for myc (NICD), Tax, or flag (FBXW7) expression. Actin served as a loading control.

stabilization of NICD (Fig. 3F). Next, we investigated whether the expression of the p100DN could be associated with a reduced binding of Tax to FBXW7.

Previous reports have shown that Tax can bind p100 (64). We found that Tax could also interact with p100DN in transient transfection assays (Fig. 4A). Next, we co-immunoprecipitated Tax and FBXW7 in the presence or absence of p100DN. These experiments showed that p100DN was unable to prevent interactions between Tax and FBXW7 (Fig. 4B). We also found that Tax could bind p100DN in the absence of FBXW7 expression (Fig. 4C). The increased amounts of FBXW7 that were immunoprecipitated when Tax was coexpressed (Fig. 4B) may be explained by the fact that Tax expression significantly increased the half-life of FBXW7 (Fig. 4D). The reasons for this increased stabilization are currently unknown and under investigation. Since p100DN was able to prevent Tax-mediated stabilization of NICD without disrupting the interactions between Tax and FBXW7, we hypothesized that p100DN might interact with the Tax/FBXW7 complex and, since p100DN cannot be processed, relocalize the Tax/FBXW7 complex to the cytoplasm. To test this hypothesis, we performed transient transfection assays and co-immunoprecipitation studies. Indeed, our studies confirmed that co-transfection of p100DN efficiently re-distributed Tax from the nucleus to the cytoplasm as demonstrated by western blot fractionation (Fig. 4E). These results were further validated by the fluorescence of GFP-Tax, which demonstrates a nuclear speckles distribution but is efficiently redistributed to the cytoplasm in the presence of p100DN (Fig. 4F). Collectively, our results demonstrate that Tax can inhibit FBXW7-mediated degradation of its targets through multiple pathways. These include direct interaction with FBXW7, preventing the recruitment of target proteins, interaction with target proteins (NICD and c-MYC), thereby preventing their binding to FBXW7, and finally, in physiological conditions where Tax is unable to process NF-κB2 p100, cytoplasmic relocalization of the Tax/FBXW7 complex by p100 preventing interaction and degradation of FBXW7 targets.

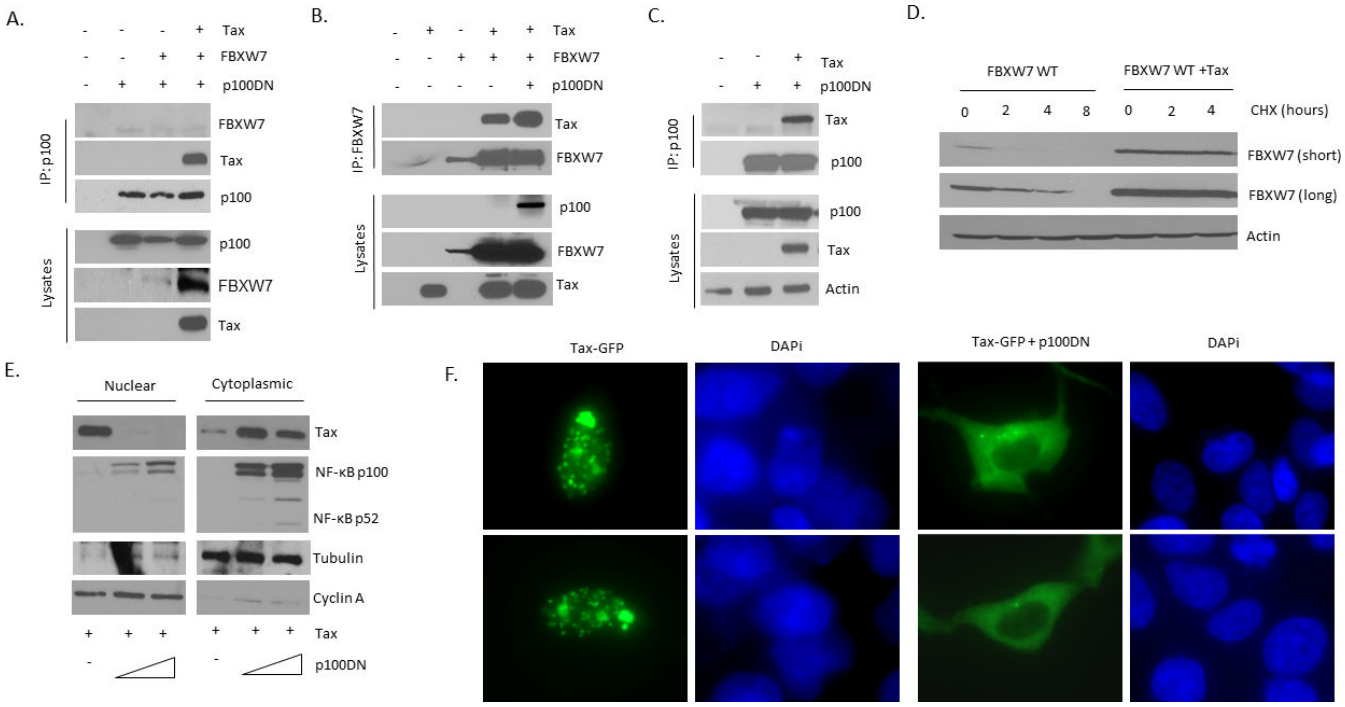

FIG 4 NF-κB2 p100 interaction with Tax can prevent FBXW7 functions. (A) NF-κB2 p100DN binds Tax. 293T cells were transfected with pcTax (1.0 µg), Flag-FBXW7 (2.0 µg), and/or p100DN (1.0 µg). Forty-eight hours later, cells were lysed in NP-40 lysis buffer and an equal amount of lysates were immunoprecipitated overnight with anti-p100, then incubated with protein A/G beads. Immunoprecipitates and cell lysates were analyzed by western blot with anti-Flag, anti-Tax, and anti-p100 antibodies. (B) p100DN cannot disrupt the Tax/FBXW7 complex. 293T cells were transfected with pcTax (2.0 µg), Flag-FBXW7 (4.0 µg), and p100DN (2.0 µg). Lysates were collected 48 hours later and incubated overnight with anti-Flag antibody, and then immunoprecipitated with protein A/G beads. Immunoprecipitates and cell lysates were analyzed by western blot analysis with anti-Flag, anti-Tax, and anti-p100/p52 antibodies. (C) Tax binds p100DN in the absence of FBXW7. 293T cells were transfected with Tax (3.0 µg) and p100DN (3.0 µg). Lysates were collected 48 hours later and incubated overnight with anti-p100/p52 antibody, and then immunoprecipitated with protein A/G beads. Immunoprecipitates and cell lysates were analyzed by western blot analysis with anti-Tax and anti-p100/p52 antibodies. (D) Tax increases the half-life of FBXW7. 293T cells were transfected with FBXW7 and pTax. Before lysis, cells were treated with cycloheximide for 0, 2, 4, or in the case of FBXW7 alone, 8 hours. Short and long exposures of FBXW7 were taken to demonstrate the effect of CHX on FBXW7 expression in the absence of Tax. Actin served as a loading control. (E) p100 redistributes Tax to the cytoplasm. 293T cells were transfected with pcTax (0.75 µg) and increasing doses of p100DN (1–2.0 µg). Forty-eight hours later, cells were lysed in hypertonic or hypotonic lysis buffers for nuclear or cytoplasmic lysates, respectively. Western blots were probed with anti-tax and anti-p100 antibodies. Cyclin A served as an internal control for the nuclear/cytoplasm fractionation. (F) GFP-Tax was expressed in the absence or presence of p100DN in 293T cells. After 48 hours, cells were fixed in PFA, stained with DAPI, and mounted for microscopy. Representative images at 40× are shown.

To demonstrate the biological significance of our findings, i.e., Tax inactivation of FBXW7, we searched for a Tax mutant that would be unable to bind to and suppress FBXW7 activities. We first tested previously characterized Tax mutants, M47, K88V, G148V, and M22 but found they could still bind to FBXW7 and prevent FBXW7-mediated degradation of NICD (data not shown). Interestingly, we discovered that a previous Tax mutant (which we designate Tax-J) (46) was unable to block FBXW7-mediated degradation of its substrates. This plasmid was derived from a Jurkat cell line, with an inducible Tax mutant (JPXM). Sequencing of Tax-J revealed three mutations in the Tax sequence when compared to the pcTax used in this study. These mutations included R222K, L308H, and a Ser63 insertion (Fig. 5A). R222K lies within the third subdomain of Tax homodimerization (residues 213–228) (65). L308H was present in the ATF/CREB activity domain of Tax, while another mutation was outside of known Tax activation and binding domains (Fig. 5A). We also sequenced the wild-type pcTax plasmid and found a methionine to isoleucine mutation at position 206 (M206I). The M206I mutation did not impact Tax activities, including HTLV-I transactivation, NF-κB activity, or inhibition of FBXW7 functions. We then focused on the Tax-J mutant and performed

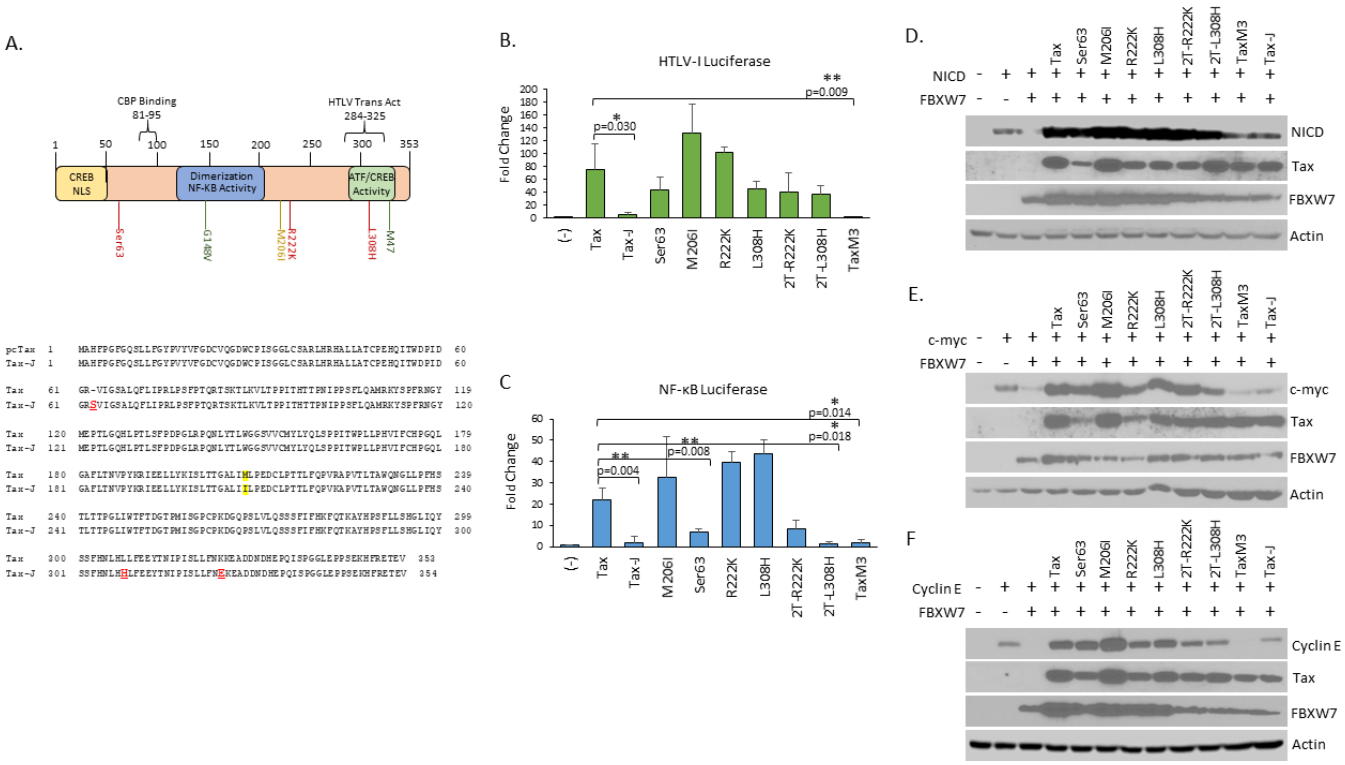

FIG 5 Tax mutant, TaxM3, is unable to stabilize FBXW7. (A) Schematic diagram of the Tax protein with positions of Tax mutations found in Tax-J noted in red. M47 and G418V are also noted. TaxM3 contains an insertion of a serine at amino acid 63 and two mutations, L308H and R222K. The M206I change was noted in the wild-type Tax protein (in yellow) but did not affect Tax functions. The alignment of pcTax and Tax-J is shown. HTLV-I transactivation and NF-κB activity of various Tax mutations found in Tax-J and TaxM3. (B and C) 293T cells were transfected with pcTax or Tax mutants (0.5 µg) along with HTLV-LTR-Luc (B) or NF-κB-Luc (C) (0.5 µg) and RLTK (0.10 µg) for 24 hours. TaxM3 denotes the Tax mutant of Ser63, R222K, and L308H. Tax mutants (Ser63 + R222K) and (Ser63 + L308H) are denoted as 2T-R222K and 2T-L308H, respectively. Luciferase measurements were taken from at least two independent experiments and were normalized to RLTK-renilla luciferase. *P*-values were indicated for significant differences in activation using the Student's *t*-test. *$P > 0.05$ and **$P > 0.01$. (D–F) The generation of Tax mutants and their effect on FBXW7 activity. 293T cells were transfected with pcTax (0.5 µg), Tax mutants (0.5 µg), Flag-FBXW7 (2.0 µg), or myc-NICD (0.16 µg) (D), HA-c-MYC (0.25 µg) (E), or myc-Cyclin E (0.10 µg) (F) for 48 hours, or in the case of Myc, 24 hours. Actin served as a loading control.

site-directed mutagenesis on wild-type Tax and made single point mutations for Ser63, R222K, and L308H, double point mutations with Ser63 with R222K (2T-R222K) or with L308H (2T-L308H), or a triple point mutant with all three mutations (TaxM3). All Tax mutants were sequenced and compared to wild-type Tax (Fig. 5A). TaxM3 lost the ability to transactivate the HTLV-I LTR (Fig. 5B). Surprisingly, no single point mutant led to an appreciable loss of Tax transactivation activity, though Ser63, L308H, and both double mutants resulted in a decrease in activity compared to the wild type (Fig. 5B). The decrease in activity with L308H is likely because this mutation lies within the Tax transactivation domain. We then examined NF-κB activation and found that like the original Tax mutant (Tax-J), Tax3M lost all ability to activate NF-κB (Fig. 5C). This is likely due to the insertion of Ser63 since a single Ser63 mutation in Tax also led to the loss of NF-κB activity, which was also seen in 2T-R222K and 2T-L308H. The loss in NF-κB activity did not appear to be due to a lower level of Tax expression since other Tax mutants expressed varying or low levels of Tax. Yet, these mutants were able to still activate HTLV-I LTR or NF-κB activity (i.e., R222K) (Fig. 5B and C). We then examined the ability of single, double, or TaxM3 mutants to inhibit FBXW7-mediated degradation of NICD (Fig. 5D), c-MYC (Fig. 5E), or Cyclin E (Fig. 5F). We found that many single and triple Tax mutants could stabilize FBXW7 targets to comparable levels as the wild-type Tax. The fact that Tax mutant Ser63 could stabilize all three substrates emphasizes that low

levels of Tax expression are sufficient and NF-κB activating function is dispensable for Tax-mediated stabilization of FBXW7 targets (Fig. 5C through F).

Importantly, TaxM3 could not inhibit FBXW7-mediated degradation of NICD, c-MYC, and Cyclin E substrates (Fig. 5D through F). Because TaxM3 expressed lower amounts of Tax compared to wild type, we repeated FBXW7-mediated degradation of NICD, c-MYC, and Cyclin E in the presence of increasing amounts of TaxM3. Even though large amounts of TaxM3 were expressed, the mutant could still not inhibit FBXW7 and stabilize NICD, c-MYC, or Cyclin E (Fig. 6A through C). We then performed similar experiments with low levels of wild-type Tax and found that even at lower levels of Tax, Tax could still inhibit FBXW7-mediated degradation of Notch (Fig. 6D). Collectively, these data suggest that we identified a Tax mutant, namely TaxM3, that is unable to prevent FBXW7-mediated degradation, and that this was not the result of lower expression levels or the inability to activate CREB or NF-κB signaling pathways. To determine why TaxM3 could no longer inhibit FBXW7, we performed immunoprecipitation with wild type or the TaxM3 mutant. In support of the above data, we found that the TaxM3 could no longer bind FBXW7 (Fig. 6E). Since TaxM3 no longer binds FBXW7, it was unnecessary to test whether this mutant also inactivates GSK3β or can still induce processing of NF-κB2 p100. Finally, to determine the importance of FBXW7 function in HTLV-1 Tax-mediated transformation, we examined the ability of TaxM3 to transform fibroblast Rat1 cells. Rat1 fibroblasts were transfected with puromycin, along with wild type or TaxM3, and grown long term in the presence of puromycin. After several weeks, distinct colonies appeared in cells expressing wild-type Tax (Fig. 6F). However, no colonies formed without Tax or with TaxM3. These data suggest that the Tax mutant, TaxM3, lost the ability to transform cells and that the inability of TaxM3 to block FBXW7-mediated degradation of key

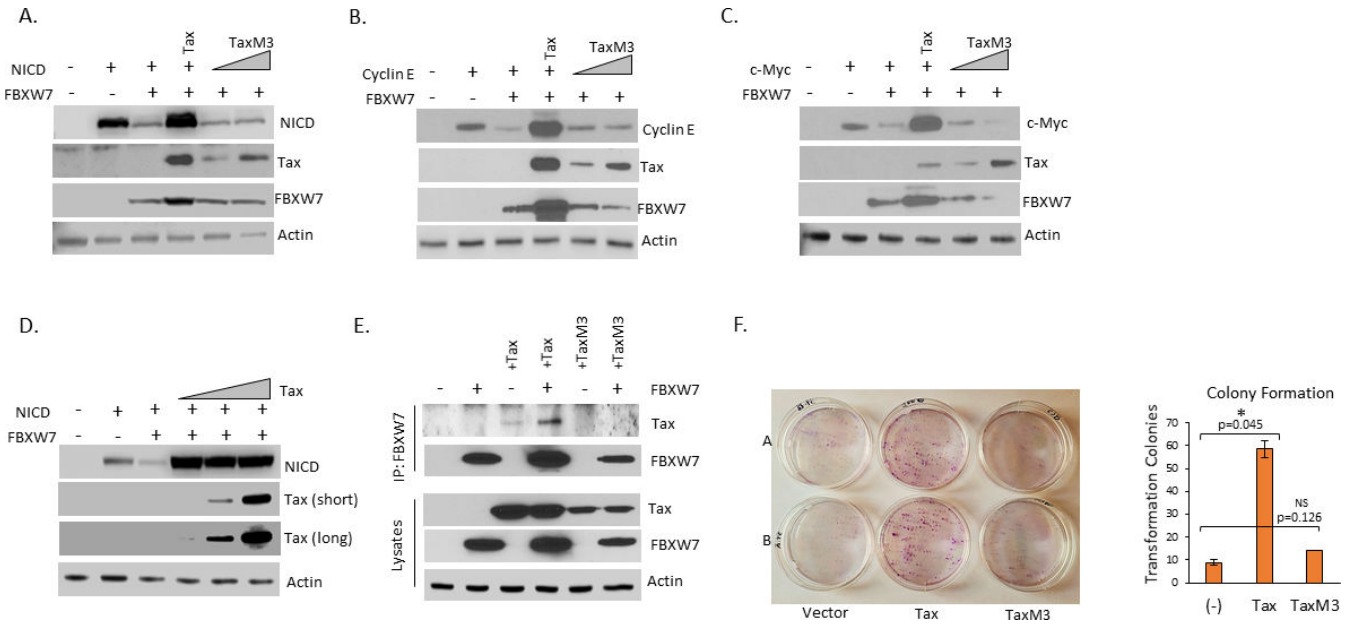

FIG 6 FBXW7-Tax mutant, TaxM3, lost the ability to transform cells. (A–D) Reduced protein expression is not the underlying cause of TaxM3's inability to inhibit FBXW7 functions. (A–C) 293T cells were transfected with pcTax or increasing amounts of TaxM3, along with 0.16 µg myc-NICD (A), 0.10 µg myc-Cyclin E (B), or 0.25 µg HA-c-Myc (C), along with 2.0 µg Flag-FBXW7 for 48 hours, or in the case of Myc, 24 hours. Actin served as a loading control. 293T were also transfected with increasing amounts of pcTax, myc-NICD, and Flag-FBXW7 (D). Tax could only be detected at low transfection amounts, yet still stabilized NICD. Actin served as a loading control. (E) TaxM3 cannot bind FBXW7. 293T cells were transfected with 2.0 µg pcTax or 4.0 µg TaxM3, along with 3.0 µg Flag-FBXW7 for 48 hours. Equal amounts of lysates were immunoprecipitated overnight with anti-Flag Ab and probed with anti-Tax. Equal amounts of lysates were loaded for controls. (F) Tax mutant, TaxM3, is unable to transform cells. Rat1 cells were transfected by calcium phosphate with 5.0 µg pcTax or TaxM3, along with 0.5 µg pSIH1-puro. Cells were cultured in the presence of puromycin for over 2 weeks. Cells were then stained for colony formation. Rat-1 colony formation was repeated at least twice, and individual colonies were counted. Results are quantified in bar graphs. *P*-values were calculated using a paired, two-tail distribution, *t*-test.

oncogenic substrates, NICD, c-MYC, Cyclin E, and Mcl-1 likely contributed to the loss of Tax transforming capabilities, in conjunction with a loss of NF-κB activation.

DISCUSSION

HTLV-I Tax has been shown to activate cellular signaling pathways (NF-κB, AKT, Notch, and hTERT), inactivate cell cycle checkpoints (Cyclin E/CDK2, Cyclin D, and p21WAF), inhibit tumor suppressors (p53, RB1, and p16ink4), and activate regulators of apoptosis (Bcl-xL and Mcl-1) (66). In addition, Tax impairs DNA replication forks, increases DSBs, and inhibits DNA repair pathways promoting the accumulation of genetic mutations. Tax is highly expressed in the early stages after infection, but its expression decreases over time and only 20% of all ATL patient samples retain Tax expression, suggesting that Tax is essential to achieve transformation but may not be required to maintain survival and expansion of transformed cells. Herein, we demonstrate that HTLV-I oncoprotein Tax inhibits the tumor suppressor FBXW7, resulting in an increased expression of NICD and other key oncogenic drivers such as c-Myc, Cyclin E, and Mcl-1. Furthermore, other targets of FBXW7 are also affected in HTLV-I cells, namely p53, mTOR, p100, and AURKA. Whether the deregulation of these proteins in HTLV-I-infected cells is related to Tax-mediated inactivation of FBXW7 and participation in the immortalization process warrants additional studies. Importantly, we also found that a Tax mutant defective in binding and inactivating FBXW7 had impaired transforming activities. This mutant was also defective in activating the HTLV-I LTR and enhancing the activation of NF-κB. Tax-mediated control of NF-κB expression and activity has been a key driver of HTLV-I-facilitated cellular transformation (53, 67). NF-κB activity is found to be constitutively active in the majority of primary ATL-transformed cells using Tax-dependent and independent mechanisms (68). Therefore, while a direct role for FBXW7 in the Tax transformation process was not determined, these observations suggest that the inactivation of FBXW7 function(s) may play a critical role in Tax-induced cellular transformation. This is especially important in light of FBXW7's role in NICD, c-Myc, cyclin E, and Mcl-1 expression. In support of this, the re-expression of wild-type FBXW7 in ATL-transformed cells leads to a considerable loss in proliferation (14).

Our studies also show that Tax led to an increase in FBXW7 protein expression levels. It will be important to know whether Tax elevates FBXW7 gene expression and protein stability, by preventing its autoubiquitination, or prevents the actions of a negative regulator of FBXW7. Non-coding RNAs such as microRNAs and long non-coding RNAs, as well as post-transcriptional regulators and processors, have been demonstrated to regulate FBXW7 protein levels, including self-ubiquitination (69, 70). When Tax binds to FBXW7, it could potentially hinder FBXW7's self-ubiquitination, causing it to accumulate by preventing proteasomal degradation (71). Tax-expressing cells have been shown to over-express peptidyl-prolyl isomerase (Pin1), which negatively regulates FBXW7 stability (71, 72). Interestingly, Pin1 is important for Tax-mediated transformation. Whether this is because of the negative function of FBXW7 warrants further studies. Interestingly, other oncogenic viruses have also been shown to play a role in FBXW7 regulation. The latent membrane protein 1 of Epstein-Barr virus has been shown to increase c-MYC expression by regulating the PI3K-AKT-GSK3β-FBXW7 pathway (73). In contrast, FBXW7 has been shown to have antiviral capabilities by binding and stabilizing RIG-I (retinoic acid-inducible gene) (74), and this explains why viruses would want to inactivate FBXW7. RIG-I is an important player in the interferon (IFN) response to viral RNA viruses, and known oncogenic viruses such as HCV (hepatitis C virus) have employed mechanisms to disrupt RIG-I functions (75–77). The nonstructural protein 2 (nsp2) of porcine epidemic diarrhea virus also mediates FBXW7 degradation, effectively disrupting the antiviral response of FBXW7 (78). Loss of FBXW7 has also been implicated in the resistance to anti-PD-1 (programmed cell death 1) therapy, through loss of RIG-I and MDA5 (interferon-induced with helicase C domain 1) sensing of dsRNA, along with decreased IFN-I and MCH-I (major histocompatibility complex) expression (79). Therefore, a better understanding of FBXW7 inactivation may help find ways to reactivate FBXW7 in tumor cells and restore

sensitivity to PD-1 therapies. HTLV-I Tax has been shown to impede RIG-I function by multiple mechanisms involving SOCS1 (suppressor of cytokine signaling) and RIPK1 (receptor interacting serine/threonine kinase1) (80). Future studies could determine if blocking FBXW7 function impairs the antiviral response in HTLV-I-infected cells. This would suggest that blocking FBXW7 would have novel functions in HTLV-I-infected cells, independent of its role in tumorigenesis. Because HTLV-I elicits vigorous immune responses and presents a low antigenic variability, reducing viral antigen expression is essential. Virus-expressing cells are rapidly eliminated by CTL activity against the highly immunogenic viral Tax protein (81, 82). While Tax expression is essential for the immortalization of human T cells, HTLV-I-transformed cells usually do not constantly express the Tax protein but rather present sporadical bursts of Tax expression (13). It would be interesting to determine if Tax re-expression blocks the antiviral activities of FBXW7. FBXW7 is also implicated in binding the nonstructural protein 5B (NS5B) of HCV (83) through a CPD sequence found in the NS5B. Consequently, forced over-expression of FBXW7 has been shown to cause a downregulation of the HCV virus. It is unknown how HCV interferes with FBXW7 function, but FBXW7 is known to be decreased in aggressive hepatocellular carcinoma and low expression correlates with poor prognosis (84).

In conclusion, we demonstrated that HTLV-I Tax, and not HBZ, can inhibit the functions of the tumor suppressor FBXW7. Tax inhibition of FBXW7 activities allows the increased expression of pro-oncogenic targets, such as Notch, c-Myc, Mcl-1, and Cyclin E. The pro-tumorigenic effect of this action is underscored by the fact that a Tax mutant (TaxM3), which is unable to inhibit FBXW7 functions and elevate NF-κB, cannot transform primary fibroblast cells.

ACKNOWLEDGMENTS

This work was supported by NIH Grant R01CA201309 and R21AI166097 and KUMED Pathology Pilot Grant GR17982 to C.N.

M.B. performed experiments, analyzed the data, and wrote the manuscript, C.Y. and X.T.B. performed experiments, and C.N. designed the study, performed experiments, analyzed data, and wrote the manuscript.

AUTHOR AFFILIATION

[1]Department of Pathology and Laboratory Medicine, University of Kansas Medical Center, Kansas City, Kansas, USA

AUTHOR ORCIDs

Christophe Nicot http://orcid.org/0000-0001-5927-2869

FUNDING

Funder	Grant(s)	Author(s)
HHS | NIH | National Cancer Institute (NCI)	R01CA201309	Christophe Nicot
HHS | NIH | National Institute of Allergy and Infectious Diseases (NIAID)	R21AI166097	Christophe Nicot

AUTHOR CONTRIBUTIONS

Marcia Bellon, Data curation, Formal analysis, Investigation, Methodology, Writing – review and editing | Chien-hung Yeh, Data curation, Investigation | Xue Tao Bai, Data curation, Investigation | Christophe Nicot, Conceptualization, Formal analysis, Funding acquisition, Investigation, Methodology, Project administration, Supervision, Writing – original draft, Writing – review and editing

DATA AVAILABILITY

Data sharing does not apply to this article as no data sets were generated or analyzed during the current study. Any plasmids generated can be obtained by contacting the corresponding author.

REFERENCES

1. Cook L, Melamed A, Yaguchi H, Bangham CR. 2017. The impact of HTLV-1 on the cellular genome. Curr Opin Virol 26:125–131. https://doi.org/10.1016/j.coviro.2017.07.013
2. Saito M. 2019. Association between HTLV-1 genotypes and risk of HAM/TSP. Front Microbiol 10:1101. https://doi.org/10.3389/fmicb.2019.01101
3. Tan BJY, Sugata K, Ono M, Satou Y. 2022. HTLV-1 persistence and leukemogenesis: a game of hide-and-seek with the host immune system. Front Immunol 13:991928. https://doi.org/10.3389/fimmu.2022.991928
4. Bellon M, Bialuk I, Galli V, Bai X-T, Farre L, Bittencourt A, Marçais A, Petrus MN, Ratner L, Waldmann TA, Asnafi V, Gessain A, Matsuoka M, Franchini G, Hermine O, Watanabe T, Nicot C. 2021. Germinal epimutation of Fragile Histidine Triad (FHIT) gene is associated with progression to acute and chronic adult T-cell leukemia diseases. Mol Cancer 20:86. https://doi.org/10.1186/s12943-021-01370-2
5. Kataoka K, Koya J. 2020. Clinical application of genomic aberrations in adult T-cell leukemia/lymphoma. J Clin Exp Hematop 60:66–72. https://doi.org/10.3960/jslrt.20019
6. Kataoka K, Nagata Y, Kitanaka A, Shiraishi Y, Shimamura T, Yasunaga J-I, Totoki Y, Chiba K, Sato-Otsubo A, Nagae G, et al. 2015. Integrated molecular analysis of adult T cell leukemia/lymphoma. Nat Genet 47:1304–1315. https://doi.org/10.1038/ng.3415
7. Mohanty S, Harhaj EW. 2020. Mechanisms of oncogenesis by HTLV-1 Tax. Pathogens 9:543. https://doi.org/10.3390/pathogens9070543
8. Bellon M, Baydoun HH, Yao Y, Nicot C. 2010. HTLV-I Tax-dependent and -independent events associated with immortalization of human primary T lymphocytes. Blood 115:2441–2448. https://doi.org/10.1182/blood-2009-08-241117
9. Nicot C. 2015. HTLV-I tax-mediated inactivation of cell cycle checkpoints and DNA repair pathways contribute to cellular transformation: "A random mutagenesis model". J Cancer Sci 2. https://doi.org/10.13188/2377-9292.1000009
10. Zhi H, Yang L, Kuo YL, Ho YK, Shih HM, Giam CZ. 2011. NF-kappaB hyper-activation by HTLV-1 tax induces cellular senescence, but can be alleviated by the viral anti-sense protein HBZ. PLoS Pathog 7:e1002025. https://doi.org/10.1371/journal.ppat.1002025
11. Baydoun HH, Bai XT, Shelton S, Nicot C. 2012. HTLV-I tax increases genetic instability by inducing DNA double strand breaks during DNA replication and switching repair to NHEJ. PLoS One 7:e42226. https://doi.org/10.1371/journal.pone.0042226
12. Mühleisen A, Giaisi M, Köhler R, Krammer PH, Li-Weber M. 2014. Tax contributes apoptosis resistance to HTLV-1-infected T cells via suppression of Bid and Bim expression. Cell Death Dis 5:e1575. https://doi.org/10.1038/cddis.2014.536
13. Mahgoub M, Yasunaga JI, Iwami S, Nakaoka S, Koizumi Y, Shimura K, Matsuoka M. 2018. Sporadic on/off switching of HTLV-1 Tax expression is crucial to maintain the whole population of virus-induced leukemic cells. Proc Natl Acad Sci U S A 115:E1269–E1278. https://doi.org/10.1073/pnas.1715724115
14. Yeh CH, Bellon M, Pancewicz-Wojtkiewicz J, Nicot C. 2016. Oncogenic mutations in the FBXW7 gene of adult T-cell leukemia patients. Proc Natl Acad Sci U S A 113:6731–6736. https://doi.org/10.1073/pnas.1601537113
15. Fan J, Bellon M, Ju M, Zhao L, Wei M, Fu L, Nicot C. 2022. Clinical significance of FBXW7 loss of function in human cancers. Mol Cancer 21:87. https://doi.org/10.1186/s12943-022-01548-2
16. Kourtis N, Strikoudis A, Aifantis I. 2015. Emerging roles for the FBXW7 ubiquitin ligase in leukemia and beyond. Curr Opin Cell Biol 37:28–34. https://doi.org/10.1016/j.ceb.2015.09.003
17. Skaar JR, Pagan JK, Pagano M. 2013. Mechanisms and function of substrate recruitment by F-box proteins. Nat Rev Mol Cell Biol 14:369–381. https://doi.org/10.1038/nrm3582
18. Yeh CH, Bellon M, Nicot C. 2018. FBXW7: a critical tumor suppressor of human cancers. Mol Cancer 17:115. https://doi.org/10.1186/s12943-018-0857-2
19. Mo J-S, Kim M-Y, Han S-O, Kim I-S, Ann E-J, Lee KS, Seo M-S, Kim J-Y, Lee S-C, Park J-W, Choi E-J, Seong JY, Joe CO, Faessler R, Park H-S. 2007. Integrin-linked kinase controls Notch1 signaling by down-regulation of protein stability through Fbw7 ubiquitin ligase. Mol Cell Biol 27:5565–5574. https://doi.org/10.1128/MCB.02372-06
20. Yeh CH, Bellon M, Wang F, Zhang H, Fu L, Nicot C. 2020. Loss of FBXW7-mediated degradation of BRAF elicits resistance to BET inhibitors in adult T cell leukemia cells. Mol Cancer 19:139. https://doi.org/10.1186/s12943-020-01254-x
21. Yada M, Hatakeyama S, Kamura T, Nishiyama M, Tsunematsu R, Imaki H, Ishida N, Okumura F, Nakayama K, Nakayama KI. 2004. Phosphorylation-dependent degradation of c-Myc is mediated by the F-box protein Fbw7. EMBO J 23:2116–2125. https://doi.org/10.1038/sj.emboj.7600217
22. Koo J, Wu X, Mao Z, Khuri FR, Sun SY. 2015. Rictor undergoes glycogen synthase kinase 3 (GSK3)-dependent, FBXW7-mediated ubiquitination and proteasomal degradation. J Biol Chem 290:14120–14129. https://doi.org/10.1074/jbc.M114.633057
23. Welcker M, Clurman BE. 2008. FBW7 ubiquitin ligase: a tumour suppressor at the crossroads of cell division, growth and differentiation. Nat Rev Cancer 8:83–93. https://doi.org/10.1038/nrc2290
24. Pancewicz J, Taylor JM, Datta A, Baydoun HH, Waldmann TA, Hermine O, Nicot C. 2010. Notch signaling contributes to proliferation and tumor formation of human T-cell leukemia virus type 1-associated adult T-cell leukemia. Proc Natl Acad Sci U S A 107:16619–16624. https://doi.org/10.1073/pnas.1010722107
25. Choi YB, Harhaj EW. 2014. HTLV-1 tax stabilizes MCL-1 via TRAF6-dependent K63-linked polyubiquitination to promote cell survival and transformation. PLoS Pathog 10:e1004458. https://doi.org/10.1371/journal.ppat.1004458
26. Wang L, Deng L, Wu K, de la Fuente C, Wang D, Kehn K, Maddukuri A, Baylor S, Santiago F, Agbottah E, Trigon S, Morange M, Mahieux R, Kashanchi F. 2002. Inhibition of HTLV-1 transcription by cyclin dependent kinase inhibitors. Mol Cell Biochem 237:137–153. https://doi.org/10.1023/a:1016555821581
27. Pise-Masison CA, Choi KS, Radonovich M, Dittmer J, Kim SJ, Brady JN. 1998. Inhibition of p53 transactivation function by the human T-cell lymphotropic virus type 1 Tax protein. J Virol 72:1165–1170. https://doi.org/10.1128/JVI.72.2.1165-1170.1998
28. O'Neil J, Grim J, Strack P, Rao S, Tibbitts D, Winter C, Hardwick J, Welcker M, Meijerink JP, Pieters R, Draetta G, Sears R, Clurman BE, Look AT. 2007. FBW7 mutations in leukemic cells mediate NOTCH pathway activation and resistance to gamma-secretase inhibitors. J Exp Med 204:1813–1824. https://doi.org/10.1084/jem.20070876
29. Bellon M, Moles R, Chaib-Mezrag H, Pancewicz J, Nicot C. 2018. JAG1 overexpression contributes to Notch1 signaling and the migration of HTLV-1-transformed ATL cells. J Hematol Oncol 11:119. https://doi.org/10.1186/s13045-018-0665-6
30. Finkin S, Aylon Y, Anzi S, Oren M, Shaulian E. 2008. Fbw7 regulates the activity of endoreduplication mediators and the p53 pathway to prevent drug-induced polyploidy. Oncogene 27:4411–4421. https://doi.org/10.1038/onc.2008.77
31. Wertz IE, Kusam S, Lam C, Okamoto T, Sandoval W, Anderson DJ, Helgason E, Ernst JA, Eby M, Liu J, et al. 2011. Sensitivity to antitubulin chemotherapeutics is regulated by MCL1 and FBW7. Nature 471:110–114. https://doi.org/10.1038/nature09779
32. Liu J, Wei L, Hu N, Wang D, Ni J, Zhang S, Liu H, Lv T, Yin J, Ye M, Song Y. 2022. FBW7-mediated ubiquitination and destruction of PD-1 protein primes sensitivity to anti-PD-1 immunotherapy in non-small cell lung

cancer. J Immunother Cancer 10:e005116. https://doi.org/10.1136/jitc-2022-005116
33. Zhang Q, Karnak D, Tan M, Lawrence TS, Morgan MA, Sun Y. 2016. FBXW7 facilitates nonhomologous end-joining via K63-linked polyubiquitylation of XRCC4. Mol Cell 61:419–433. https://doi.org/10.1016/j.molcel.2015.12.010
34. Lan H, Sun Y. 2021. Tumor suppressor FBXW7 and its regulation of DNA damage response and repair. Front Cell Dev Biol 9:751574. https://doi.org/10.3389/fcell.2021.751574
35. Takada M, Zhang W, Suzuki A, Kuroda TS, Yu Z, Inuzuka H, Gao D, Wan L, Zhuang M, Hu L, Zhai B, Fry CJ, Bloom K, Li G, Karpen GH, Wei W, Zhang Q. 2017. FBW7 loss promotes chromosomal instability and tumorigenesis via cyclin E1/CDK2-mediated phosphorylation of CENP-A. Cancer Res 77:4881–4893. https://doi.org/10.1158/0008-5472.CAN-17-1240
36. Pumfery A, de la Fuente C, Kashanchi F. 2006. HTLV-1 Tax: centrosome amplification and cancer. Retrovirology 3:50. https://doi.org/10.1186/1742-4690-3-50
37. Chaib-Mezrag H, Lemaçon D, Fontaine H, Bellon M, Bai XT, Drac M, Coquelle A, Nicot C. 2014. Tax impairs DNA replication forks and increases DNA breaks in specific oncogenic genome regions. Mol Cancer 13:205. https://doi.org/10.1186/1476-4598-13-205
38. Harada S, Koyanagi Y, Yamamoto N. 1985. Infection of human T-lymphotropic virus type-1 (HTLV-I)-bearing MT-4 cells with HTLV-III (AIDS virus): chronological studies of early events. Virology 146:272–281. https://doi.org/10.1016/0042-6822(85)90010-8
39. Salahuddin SZ, Markham PD, Wong-Staal F, Franchini G, Kalyanaraman VS, Gallo RC. 1983. Restricted expression of human T-cell leukemia--lymphoma virus (HTLV) in transformed human umbilical cord blood lymphocytes. Virology 129:51–64. https://doi.org/10.1016/0042-6822(83)90395-1
40. Popovic M, Sarin PS, Robert-Gurroff M, Kalyanaraman VS, Mann D, Minowada J, Gallo RC. 1983. Isolation and transmission of human retrovirus (human t-cell leukemia virus). Science 219:856–859. https://doi.org/10.1126/science.6600519
41. Sun SC, Ganchi PA, Ballard DW, Greene WC. 1993. NF-kappa B controls expression of inhibitor I kappa B alpha: evidence for an inducible autoregulatory pathway. Science 259:1912–1915. https://doi.org/10.1126/science.8096091
42. Xiao G, Cvijic ME, Fong A, Harhaj EW, Uhlik MT, Waterfield M, Sun SC. 2001. Retroviral oncoprotein Tax induces processing of NF-kappaB2/p100 in T cells: evidence for the involvement of IKKalpha. EMBO J 20:6805–6815. https://doi.org/10.1093/emboj/20.23.6805
43. Ganchi PA, Sun SC, Greene WC, Ballard DW. 1992. I kappa B/MAD-3 masks the nuclear localization signal of NF-kappa B p65 and requires the transactivation domain to inhibit NF-kappa B p65 DNA binding. Mol Biol Cell 3:1339–1352. https://doi.org/10.1091/mbc.3.12.1339
44. Shembade N, Harhaj NS, Yamamoto M, Akira S, Harhaj EW. 2007. The human T-cell leukemia virus type 1 Tax oncoprotein requires the ubiquitin-conjugating enzyme Ubc13 for NF-kappaB activation. J Virol 81:13735–13742. https://doi.org/10.1128/JVI.01790-07
45. Meertens L, Chevalier S, Weil R, Gessain A, Mahieux R. 2004. A 10-amino acid domain within human T-cell leukemia virus type 1 and type 2 tax protein sequences is responsible for their divergent subcellular distribution. J Biol Chem 279:43307–43320. https://doi.org/10.1074/jbc.M400497200
46. Ichikawa T, Nakahata S, Fujii M, Iha H, Shimoda K, Morishita K. 2019. The regulation of NDRG2 expression during ATLL development after HTLV-1 infection. Biochim Biophys Acta Mol Basis Dis 1865:2633–2646. https://doi.org/10.1016/j.bbadis.2019.07.001
47. Sun SC, Elwood J, Béraud C, Greene WC. 1994. Human T-cell leukemia virus type I Tax activation of NF-kappa B/Rel involves phosphorylation and degradation of I kappa B alpha and RelA (p65)-mediated induction of the c-rel gene. Mol Cell Biol 14:7377–7384. https://doi.org/10.1128/mcb.14.11.7377-7384.1994
48. Xiao G, Harhaj EW, Sun SC. 2000. Domain-specific interaction with the I kappa B kinase (IKK)regulatory subunit IKK gamma is an essential step in tax-mediated activation of IKK. J Biol Chem 275:34060–34067. https://doi.org/10.1074/jbc.M002970200
49. Kar R, Jha SK, Ojha S, Sharma A, Dholpuria S, Raju VSR, Prasher P, Chellappan DK, Gupta G, Kumar Singh S, Paudel KR, Hansbro PM, Kumar Singh S, Ruokolainen J, Kesari KK, Dua K, Jha NK. 2021. The FBXW7-NOTCH interactome: a ubiquitin proteasomal system-induced crosstalk modulating oncogenic transformation in human tissues. Cancer Rep (Hoboken) 4:e1369. https://doi.org/10.1002/cnr2.1369
50. Cherian MA, Baydoun HH, Al-Saleem J, Shkriabai N, Kvaratskhelia M, Green P, Ratner L. 2015. Akt pathway activation by human T-cell leukemia virus type 1 Tax oncoprotein. J Biol Chem 290:26270–26281. https://doi.org/10.1074/jbc.M115.684746
51. Bellon M, Ko NL, Lee MJ, Yao Y, Waldmann TA, Trepel JB, Nicot C. 2013. Adult T-cell leukemia cells overexpress Wnt5a and promote osteoclast differentiation. Blood 121:5045–5054. https://doi.org/10.1182/blood-2012-07-439109
52. Nicot C, Mahieux R, Opavsky R, Cereseto A, Wolff L, Brady JN, Franchini G. 2000. HTLV-I Tax transrepresses the human c-Myb promoter independently of its interaction with CBP or p300. Oncogene 19:2155–2164. https://doi.org/10.1038/sj.onc.1203536
53. Harhaj EW, Giam C-Z. 2018. NF-kappaB signaling mechanisms in HTLV-1-induced adult T-cell leukemia/lymphoma. FEBS J 285:3324–3336. https://doi.org/10.1111/febs.14492
54. Smith MR, Greene WC. 1990. Identification of HTLV-I tax trans-activator mutants exhibiting novel transcriptional phenotypes. Genes Dev 4:1875–1885. https://doi.org/10.1101/gad.4.11.1875
55. Yamaoka S, Inoue H, Sakurai M, Sugiyama T, Hazama M, Yamada T, Hatanaka M. 1996. Constitutive activation of NF-kappa B is essential for transformation of rat fibroblasts by the human T-cell leukemia virus type I Tax protein. EMBO J 15:873–887. https://doi.org/10.1002/j.1460-2075.1996.tb00422.x
56. Cheng W, Zheng T, Wang Y, Cai K, Wu W, Zhao T, Xu R. 2019. Activation of Notch1 signaling by HTLV-1 Tax promotes proliferation of adult T-cell leukemia cells. Biochem Biophys Res Commun 512:598–603. https://doi.org/10.1016/j.bbrc.2019.03.094
57. Saito K, Saito M, Taniura N, Okuwa T, Ohara Y. 2010. Activation of the PI3K-Akt pathway by human T cell leukemia virus type 1 (HTLV-1) oncoprotein Tax increases Bcl3 expression, which is associated with enhanced growth of HTLV-1-infected T cells. Virology 403:173–180. https://doi.org/10.1016/j.virol.2010.04.018
58. Lanoix J, Lacoste J, Pepin N, Rice N, Hiscott J. 1994. Overproduction of NFKB2 (lyt-10) and c-Rel: a mechanism for HTLV-I Tax-mediated transactivation via the NF-kappa B signalling pathway. Oncogene 9:841–852.
59. Fochi S, Mutascio S, Bertazzoni U, Zipeto D, Romanelli MG. 2018. HTLV deregulation of the NF-kappaB pathway: an update on Tax and antisense proteins role. Front Microbiol 9:285. https://doi.org/10.3389/fmicb.2018.00285
60. Kfoury Y, Nasr R, Favre-Bonvin A, El-Sabban M, Renault N, Giron M-L, Setterblad N, Hajj HE, Chiari E, Mikati AG, Hermine O, Saib A, de Thé H, Pique C, Bazarbachi A. 2008. Ubiquitylated Tax targets and binds the IKK signalosome at the centrosome. Oncogene 27:1665–1676. https://doi.org/10.1038/sj.onc.1210804
61. Sinha-Datta U, Horikawa I, Michishita E, Datta A, Sigler-Nicot JC, Brown M, Kazanji M, Barrett JC, Nicot C. 2004. Transcriptional activation of hTERT through the NF-kappaB pathway in HTLV-I-transformed cells. Blood 104:2523–2531. https://doi.org/10.1182/blood-2003-12-4251
62. Chen L, Mu Y, Greene WC. 2002. Acetylation of RelA at discrete sites regulates distinct nuclear functions of NF-kappaB. EMBO J 21:6539–6548. https://doi.org/10.1093/emboj/cdf660
63. Xiao G, Harhaj EW, Sun SC. 2001. NF-kappaB-inducing kinase regulates the processing of NF-kappaB2 p100. Mol Cell 7:401–409. https://doi.org/10.1016/s1097-2765(01)00187-3
64. Murakami T, Hirai H, Suzuki T, Fujisawa J, Yoshida M. 1995. HTLV-1 Tax enhances NF-kappa B2 expression and binds to the products p52 and p100, but does not suppress the inhibitory function of p100. Virology 206:1066–1074. https://doi.org/10.1006/viro.1995.1029
65. Basbous J, Bazarbachi A, Granier C, Devaux C, Mesnard JM. 2003. The central region of human T-cell leukemia virus type 1 Tax protein contains distinct domains involved in subunit dimerization. J Virol 77:13028–13035. https://doi.org/10.1128/jvi.77.24.13028-13035.2003
66. Mahieux R, Pise-Masison CA, Nicot C, Green P, Hall WW, Brady JN. 2000. Inactivation of p53 by HTLV type 1 and HTLV type 2 Tax trans-activators. AIDS Res Hum Retroviruses 16:1677–1681. https://doi.org/10.1089/08892220050193137
67. Ernzen KJ, Panfil AR. 2022. Regulation of HTLV-1 transformation. Biosci Rep 42:BSR20211921. https://doi.org/10.1042/BSR20211921

68. Mori N, Fujii M, Ikeda S, Yamada Y, Tomonaga M, Ballard DW, Yamamoto N. 1999. Constitutive activation of NF-kappaB in primary adult T-cell leukemia cells. Blood 93:2360–2368.
69. Jiménez-Izquierdo R, Morrugares R, Suanes-Cobos L, Correa-Sáez A, Garrido-Rodríguez M, Cerero-Tejero L, Khan OM, de la Luna S, Sancho R, Calzado MA. 2023. FBXW7 tumor suppressor regulation by dualspecificity tyrosine-regulated kinase 2. Cell Death Dis 14:202. https://doi.org/10.1038/s41419-023-05724-0
70. Shimizu K, Nihira NT, Inuzuka H, Wei W. 2018. Physiological functions of FBW7 in cancer and metabolism. Cell Signal 46:15–22. https://doi.org/10.1016/j.cellsig.2018.02.009
71. Min S-H, Lau AW, Lee TH, Inuzuka H, Wei S, Huang P, Shaik S, Lee DY, Finn G, Balastik M, Chen C-H, Luo M, Tron AE, Decaprio JA, Zhou XZ, Wei W, Lu KP. 2012. Negative regulation of the stability and tumor suppressor function of Fbw7 by the Pin1 prolyl isomerase. Mol Cell 46:771–783. https://doi.org/10.1016/j.molcel.2012.04.012
72. Jeong SJ, Ryo A, Yamamoto N. 2009. The prolyl isomerase Pin1 stabilizes the human T-cell leukemia virus type 1 (HTLV-1) Tax oncoprotein and promotes malignant transformation. Biochem Biophys Res Commun 381:294–299. https://doi.org/10.1016/j.bbrc.2009.02.024
73. Hu J, Li Y, Li H, Shi F, Xie L, Zhao L, Tang M, Luo X, Jia W, Fan J, Zhou J, Gao Q, Qiu S, Wu W, Zhang X, Liao W, Bode AM, Cao Y. 2022. Targeting Epstein-Barr virus oncoprotein LMP1-mediated high oxidative stress suppresses EBV lytic reactivation and sensitizes tumors to radiation therapy (vol 10, pg 11921, 2020). Theranostics 12:3609–3609. https://doi.org/10.7150/thno.73630
74. Song Y, Lai L, Chong Z, He J, Zhang Y, Xue Y, Xie Y, Chen S, Dong P, Chen L, Chen Z, Dai F, Wan X, Xiao P, Cao X, Liu Y, Wang Q. 2017. E3 ligase FBXW7 is critical for RIG-I stabilization during antiviral responses. Nat Commun 8:14654. https://doi.org/10.1038/ncomms14654
75. Liu HM, Gale M. 2010. Hepatitis C virus evasion from RIG-I-dependent hepatic innate immunity. Gastroenterol Res Pract 2010:548390. https://doi.org/10.1155/2010/548390
76. Liu Y, Olagnier D, Lin R. 2016. Host and viral modulation of RIG-I-mediated antiviral immunity. Front Immunol 7:662. https://doi.org/10.3389/fimmu.2016.00662
77. Gale M, Foy EM. 2005. Evasion of intracellular host defence by hepatitis C virus. Nature 436:939–945. https://doi.org/10.1038/nature04078
78. Li M, Wu Y, Chen J, Shi H, Ji Z, Zhang X, Shi D, Liu J, Tian J, Wang X, Shi Z, Zhang H, Zhang H, Guo L, Feng L. 2022. Innate immune evasion of porcine epidemic diarrhea virus through degradation of the FBXW7 protein via the ubiquitin-proteasome pathway. J Virol 96:e0088921. https://doi.org/10.1128/JVI.00889-21
79. Gstalder C, Liu D, Miao D, Lutterbach B, DeVine AL, Lin C, Shettigar M, Pancholi P, Buchbinder EI, Carter SL, Manos MP, Rojas-Rudilla V, Brennick R, Gjini E, Chen P-H, Lako A, Rodig S, Yoon CH, Freeman GJ, Barbie DA, Hodi FS, Miles W, Van Allen EM, Haq R. 2020. Inactivation of Fbxw7 impairs dsRNA sensing and confers resistance to PD-1 blockade. Cancer Discov 10:1296–1311. https://doi.org/10.1158/2159-8290.CD-19-1416
80. Mohanty S, Harhaj EW. 2023. Mechanisms of innate immune sensing of HTLV-1 and viral immune evasion. Pathogens 12:735. https://doi.org/10.3390/pathogens12050735
81. Masaki A, Ishida T, Suzuki S, Ito A, Mori F, Sato F, Narita T, Yamada T, Ri M, Kusumoto S, Komatsu H, Tanaka Y, Niimi A, Inagaki H, Iida S, Ueda R. 2013. Autologous Tax-specific CTL therapy in a primary adult T cell leukemia/lymphoma cell-bearing NOD/Shi-scid, IL-2Rgammanull mouse model. J Immunol 191:135–144. https://doi.org/10.4049/jimmunol.1202692
82. Kannagi M, Harada S, Maruyama I, Inoko H, Igarashi H, Kuwashima G, Sato S, Morita M, Kidokoro M, Sugimoto M. 1991. Predominant recognition of human T cell leukemia virus type I (HTLV-I) pX gene products by human CD8+ cytotoxic T cells directed against HTLV-I-infected cells. Int Immunol 3:761–767. https://doi.org/10.1093/intimm/3.8.761
83. Chen J, Wu X, Chen S, Chen S, Xiang N, Chen Y, Guo D. 2016. Ubiquitin ligase Fbw7 restricts the replication of hepatitis C virus by targeting NS5B for ubiquitination and degradation. Biochem Biophys Res Commun470:697–703. https://doi.org/10.1016/j.bbrc.2016.01.076
84. Imura S, Tovuu L-O, Utsunomiya T, Morine Y, Ikemoto T, Arakawa Y, Kanamoto M, Iwahashi S, Saito Y, Takasu C, Yamada S, Ishikawa D, Bando Y, Shimada M. 2014. Role of Fbxw7 expression in hepatocellular carcinoma and adjacent non-tumor liver tissue. J Gastroenterol Hepatol 29:1822–1829. https://doi.org/10.1111/jgh.12623